

# Kohn-Sham approach to Fermi gas superfluidity: the bilayer of fermionic polar molecules

Francesco Ancilotto<sup>1,2</sup>

<sup>1</sup>*Dipartimento di Fisica e Astronomia "Galileo Galilei" and CNISM,  
Università di Padova, via Marzolo 8, 35122 Padova, Italy*

<sup>2</sup>*CNR-IOM Democritos, via Bonomea, 265 - 34136 Trieste, Italy*

By using a well established 'ab initio' theoretical approach developed in the past to quantitatively study the superconductivity of condensed matter systems, based on the Kohn-Sham Density Functional theory, I study the superfluid properties and the BCS-BEC crossover of two parallel bi-dimensional layers of fermionic dipolar molecules, where the pairing mechanism leading to superfluidity is provided by the inter-layer coupling between dipoles. The finite temperature superfluid properties of both the homogeneous system and one were the fermions in each layer are confined by a square optical lattice are studied at half filling conditions, and for different values of the strength of the confining optical potential. The  $T=0$  results for the homogeneous system are found to be in excellent agreement with Diffusion Monte Carlo results. The superfluid transition temperature in the BCS region is found to increase, for a given inter-layer coupling, with the strength of the confining optical potential. A transition occurs at sufficiently small interlayer distances, where the fermions becomes localized within the optical lattice sites in a square geometry with an increased effective lattice constant, forming a system of localized composite bosons. This transition should be signalled by a sudden drop in the superfluid fraction of the system.

PACS numbers: 03.75.-b;67.85.-d;67.85.De

## I. INTRODUCTION

The study of superfluidity in Fermi systems is a very attractive area of research in the field of ultracold atoms because of the direct implications for superconductivity in solid-state materials as well as for nuclear and quark matter[1]. One of the most relevant experimental result in this field has been the realization, obtained by tuning the inter-particle interaction via the use of Fano-Feshbach resonances, of the crossover from the Bardeen-Cooper-Schrieffer (BCS) superfluid phase of loosely bound fermion pairs to the Bose-Einstein condensate (BEC) of tightly bound composite bosons [2, 3].

Of particular relevance are the studies aimed at understanding the pairing of fermions in strongly interacting two-dimensional (2D) Fermi gases, a subject again of great importance for condensed matter physics in view of the not yet fully understood character of the corresponding mechanism in high-temperature (layered) superconductors. While charge transport within layers plays an essential role in superconductivity of high  $T_c$  material, the long-range nature of the interactions among the particles (electrons/holes) belonging to adjacent layers is believed to largely affect the value of the critical temperature. A bilayer of fermionic particles interacting via long-range potential thus represents an excellent platform to simulate the interplay between these effects in the properties of high  $T_c$  superconductors.

Recently, the creation of ultracold dipolar gases of fermionic molecules with large intrinsic dipole moments has been achieved[4, 5], opening the way to explore the fascinating many-body physics of correlated Fermi

systems associated with the long-range, anisotropic nature of dipolar interaction between molecules[6–8], which include topological superfluidity[9, 10], interlayer pairing between two dimensional systems and the formation of dipolar quantum crystals[11] and possibly stripe phases[12].

Two-dimensional (2D) dipolar systems are of particular interest, since the lifetime of heteronuclear molecules with permanent electric dipole moment is increased by the effect of 2D confinement[13]. Indeed such polar molecules can have very large dipole moments, of the order of 1 Debye, allowing to access the regime of strong correlations in a controllable way.

When a bilayer of 2D fermionic dipoles is formed, where the dipoles in each layer are aligned perpendicularly to the planes by an external field, in spite of the repulsive interaction between fermions belonging to the same layer, a superfluid behavior is nonetheless expected, the pairing among fermions being provided by the attractive head-to-tail dipolar interaction between fermions belonging to different layers, which results in a two-body bound state for any value of the bilayer separation [14–16]. The resulting coupling is predicted to cause superfluid behavior at sufficiently low temperatures[17–20]. Moreover, a cross-over is expected by varying the inter-layer distance, as the system evolves from the weak-coupling BCS regime of largely overlapping Cooper pairs to the strong-coupling BEC regime of composite bosons[21, 22]. Additional interest in bilayers of fermions is due to the strong analogies with the physics of electron-hole bilayers in semiconductor heterostructures[23]. The BCS-BEC crossover in a (homogeneous) bilayer of fermionic dipoles has been recently

studied at zero-temperature by means of Diffusion Monte Carlo (DMC) simulations[24].

Density Functional Theory (DFT) for electrons, which is perhaps the most widely used and successful technique in electronic structure calculations of condensed matter systems, has been proposed only recently [25–27] as a useful computational tool in the field of cold gases. The main advantage of the method is that it allows to go beyond the mean-field level by taking into account correlation effects, and thus represents a valid alternative to more microscopic (but also computationally more demanding) approaches such as Quantum Monte Carlo (QMC), especially for extended and/or inhomogeneous systems.

A modified DFT approach, which has been used to study the properties of a unitary Fermi gas[26], is based on a functional form which exploits the scale invariance of the unitary regime. DFT approaches have been used recently to describe a Fermi dipolar system in various "single-orbital" approximations (Thomas-Fermi [28], Thomas-Fermi-Dirac [29], Thomas-Fermi-von Weizsacker [30, 31]). In Ref.[32] a parameter-dependent DFT-LDA approach was used to study small number of harmonically trapped fermions.

The well-known Kohn-Sham (KS) mapping[33] of the many-body problem into a non-interacting one makes the DFT approach applicable in practice, either within the Local Density Approximation (LDA) or by including suitable gradient corrections. The KS-DFT approach does not require adjustable parameters, and thus belongs to the family of the so-called 'ab initio' methods well known in the electronic structure community. Recently, the KS-DFT method has been applied to cold atomic Fermi gases in optical lattices[25, 34], the unitary trapped Bose gas [35] and to the study of a rotating dipolar Fermi gas[36].

The extension of multi-orbital KS-DFT approaches to superfluids is a challenging goal, opening important new perspectives in the theory of cold quantum gases. A formally exact generalization of "normal-state" DFT for condensed matter systems which explicitly includes in its formulation the superconducting order parameter has been proposed to describe solid-state BCS superconductors [37], and was found to be able to accurately predict experimental properties of superconducting materials, especially for systems where a theory beyond simple BCS superconductivity is needed.

I will use here a method based on the approach described in Ref.[37] to study the superfluid behavior of a homogeneous bilayer of (polarized) dipolar fermionic molecules, for which accurate  $T=0$  results exist to compare with, obtained by using QMC simulations[24]. To underline the capabilities of the method to treat in particular inhomogeneous systems (which are often difficult to study using QMC methods), I will also calculate the finite-temperature superfluid properties of this system in the presence of an additional external poten-

tial which simulates an optical 2D square lattice acting on the dipoles in each layer. I will compute, throughout the BCS-BEC crossover, the normal-state density, the superconducting gap, the condensate fraction and the superfluid transition temperature, and their changes as a function of the interlayer distances and the depth of the confining optical potential wells. The exchange-correlation energy of the homogeneous system, which is an essential ingredient of the KS-DFT method, will be provided by virtually exact Diffusion Monte Carlo calculations[24, 38].

## II. METHOD

The two-dimensional, spin-polarized dipolar Fermi gas is characterized by the (intra-layer) interaction  $V = \sum_{i<j}^N \frac{d^2}{|\mathbf{r}_i - \mathbf{r}_j|^3}$ . Here  $d$  is the electric dipole moment of an atom/molecule and  $\mathbf{r}_i, \mathbf{r}_j$  are coordinates in the 2D  $x - y$  plane. Being the dipole moments aligned parallel to the  $z$ -axis, the pair potential is purely repulsive. The range of the dipole-dipole interaction is characterized by the length  $r_0 = Md^2/\hbar^2$ ,  $M$  being the particle mass. The adimensional interaction strength characterizing the system is  $k_F r_0$  (where  $k_F = \sqrt{4\pi n}$  is the Fermi wavevector of the 2D uniform system at a density  $n$ ).

The inter-layer interaction is given by

$$V_{IL}(r, \lambda) = d^2 \frac{r^2 - 2\lambda^2}{(r^2 + \lambda^2)^{5/2}} \quad (1)$$

where  $\lambda$  is the separation between the two layers and  $r$  is the in-plane distance between two dipoles belonging to different layers. At variance with the always repulsive intra-layer interaction, the potential  $V_{IL}(r)$  is attractive for  $r < \sqrt{2}\lambda$ .

## IIA. NORMAL STATE CALCULATIONS

Within the Kohn-Sham formulation[33] of Density Functional Theory [39] for an inhomogeneous system of  $N$  interacting particles with mass  $M$ , the total energy of the system is given by the following total energy functional of the density  $n$ , which includes the exact kinetic energy of a fictitious non-interacting system and the interaction energy functional  $E_{int}$ :

$$E_{KS}[n(\mathbf{r})] = -\frac{\hbar^2}{2M} \sum_i \int \phi_i^*(\mathbf{r}) \nabla^2 \phi_i(\mathbf{r}) d\mathbf{r} + E_{int}[n(\mathbf{r})] \quad (2)$$

In the usual KS-DFT scheme for electronic systems,  $E_{int}$  is usually split into three contributions, i.e. the Hartree ("mean-field"), exchange and correlation terms.

The  $\{\phi_i(\mathbf{r}), i = 1, N\}$  are single-particle orbitals, forming an orthonormal set,  $\langle \phi_i | \phi_j \rangle = \delta_{ij}$ . I assume here a fully balanced system, with  $N$  fermions per each layer. The total density of the system is  $n(\mathbf{r}) = \sum_{i=1}^N |\phi_i(\mathbf{r})|^2$ .

In the present case a more convenient partition is  $E_{int}[n] = E_L[n] + E_{IL}[n]$ .  $E_L$  is the energy contribution due to intra-layer interactions, given by the sum of the direct+exchange interaction term (the "Hartree-Fock" energy,  $E_{HF}$ ) and the correlation energy  $E_C$ , which I write here in the Local Density Approximation[36]:

$$E_L[n] = E_{HF}[n] + E_C[n] \\ = \int \left[ \frac{256}{45} d^2 \sqrt{\pi} n(\mathbf{r})^{5/2} + n(\mathbf{r}) \epsilon_C(n(\mathbf{r})) \right] d\mathbf{r} \quad (3)$$

where  $\epsilon_C(n)$  is the correlation energy per particle of the *homogeneous* system of density  $n$ , as obtained from the (virtually exact) Diffusion Monte Carlo calculations of Ref.[38]. The actual analytical form of the function  $\epsilon_C(n)$  used to fit the DMC results is taken from Ref.32.

The inter-layer interaction energy  $E_{IL}$  is given by the sum of the Hartree term plus the correlation energy (I neglect here any exchange interaction contribution since orbitals of fermions on different layers have zero overlap):

$$E_{IL}[n] = \frac{1}{2} \int d\mathbf{r} \int d\mathbf{r}' n(\mathbf{r}) n(\mathbf{r}') V_{IL}(|\mathbf{r} - \mathbf{r}'|) + \tilde{E}_C[n] \quad (4)$$

Note that, from Eq.(1),  $\int V_{IL}(r) d\mathbf{r} = 0$  [18], i.e. the mean-field interaction energy between two layers in the homogeneous case ( $n(\mathbf{r}) = n$ ) is zero. Corrections to the mean-field approximation for the inter-layer interaction energy are incorporated in the correlation energy functional  $\tilde{E}_C$ . Informations about this term come from the results of DMC calculations for the homogeneous bilayer system[24], where the corrections to mean-field results have been computed as a function of  $k_F \lambda$  (see Fig.(3) in Ref.24). These corrections (once the energy of a single-layer dipolar Fermi liquid,  $E/N = 0.6931 \epsilon_F$  [38], has been subtracted from the DMC results) can be written in the form:

$$\tilde{E}_C/N = -\frac{\epsilon_F}{2} f(k_F \lambda) \quad (5)$$

where the function  $f$  interpolates the DMC results. I choose here  $f(x) = 0.292[1 - \tanh[5.5(x - 0.45)]]$ , which gives a reasonable overall fit to the DMC data. The above result, which holds for the homogeneous system, can be used for inhomogeneous systems as well by using again the LDA:

$$\tilde{E}_C[n] = -\frac{1}{2} \int d\mathbf{r} n(\mathbf{r}) \epsilon_F(\mathbf{r}) f(k_F(\mathbf{r}) \lambda) \quad (6)$$

where  $k_F(\mathbf{r}) \equiv \sqrt{4\pi n(\mathbf{r})}$  and  $\epsilon(\mathbf{r}) \equiv \hbar^2 k_F(\mathbf{r})^2 / 2M$  are the local values of the Fermi wave vector and energy, respectively.

The effective potential  $\mu_{IL}(\mathbf{r}) \equiv \frac{\delta E_{IL}}{\delta n}$  associated with the inter-layer interactions is thus

$$\mu_{IL}(\mathbf{r}) = \int d\mathbf{r}' n(\mathbf{r}') V_{IL}(|\mathbf{r} - \mathbf{r}'|) \\ - \frac{\epsilon_F(\mathbf{r})}{2} [2f(k_F(\mathbf{r}) \lambda) + n(\mathbf{r}) \frac{\partial f}{\partial n}] \quad (7)$$

Constrained minimization of the energy functional  $E_{KS}[n]$  leads to the coupled KS eigenvalues equations

$$\left[ -\frac{\hbar^2}{2M} \nabla^2 + V_{KS}(\mathbf{r}) \right] \phi_i(\mathbf{r}) = \epsilon_i \phi_i(\mathbf{r}) \quad (8)$$

where

$$V_{KS}(\mathbf{r}) = \epsilon_C(n(\mathbf{r})) + n(\mathbf{r}) \frac{\partial \epsilon_C}{\partial n} \\ + \frac{128}{9} d^2 \sqrt{\pi} n^{3/2}(\mathbf{r}) + \mu_{IL}(\mathbf{r}) \quad (9)$$

Solutions of the above system of equations provide the density  $n(\mathbf{r})$  (and thus the total energy, through Eq.(2)) of the fermion system in its (normal) ground-state.

In practice, the solutions  $\{\phi_i(\mathbf{r})\}$  of Eq.(8) are found by propagating in imaginary time the time-dependent version[33] of the KS equations (8) (for more details about the actual method used to efficiently propagate the orbitals  $\phi_i$  in imaginary time, see Ref.40). Both the density and the single-particle orbitals  $\phi_i$  have been discretized in cartesian coordinates using a spatial grid fine enough to guarantee well converged values of the total energy. The orthogonality between different orbitals has been enforced by a Gram-Schmidt (G-S) process. The spatial derivatives entering Eq.(8) have been calculated with accurate 13-point formulas, while efficient Fast-Fourier techniques[41] have been used to calculate the non-local term entering the KS potential  $V_{KS}$  and the potential term entering the gap equation (see the following Section).

## IIB. SUPERFLUID STATE CALCULATIONS

The basic formulation of the KS-DFT for superconductors[37], which I will follow, *mutatis mutandis*, in the present work, is described in the following.

The theory is based on the fermion (electron) density  $n(\mathbf{r}) = \langle \Psi^\dagger(\mathbf{r}) \Psi(\mathbf{r}) \rangle$  ("normal" density) as well as the superconducting order parameter ("anomalous" density)  $\chi(\mathbf{r}, \mathbf{r}') = \langle \Psi(\mathbf{r}) \Psi(\mathbf{r}') \rangle$  where  $\Psi^\dagger(\mathbf{r})$  is the fermion creation operator. This quantity is finite for superconductors below the transition temperature and zero above

it. Associated to these two densities there are two key quantities, i.e. the KS potential  $V_{KS}(\mathbf{r})$  described in the previous Section, and the so-called anomalous potential  $\Delta_s(\mathbf{r}, \mathbf{r}')$ :

$$\Delta_s(\mathbf{r}, \mathbf{r}') = \chi(\mathbf{r}, \mathbf{r}')V(|\mathbf{r} - \mathbf{r}'|) + \Delta_{xc}(\mathbf{r}, \mathbf{r}') \quad (10)$$

Here  $V(|\mathbf{r} - \mathbf{r}'|)$  represents the effective interaction between the fermionic particles responsible for pairing. In the present case  $V \equiv V_{IL}$ , where  $V_{IL}$  is the inter-layer dipole-dipole interaction potential, Eq.(1). The first term in Eq.(10) corresponds to the Hartree (mean-field) approximation, while the extra term include exchange and correlation effects. Although recipes have been proposed to approximately construct  $\Delta_{xc}$  for electronic superconductors[37], which may be adapted to the case of fermionic cold gases, I neglect it here because in the present case the attractive interaction acts between fermions belonging to different, spatially separated 2D layers, and thus exchange is null. I am nevertheless including neglected correlation effects beyond mean-field in the chemical potential (7).

The Kohn-Sham Bogoliubov-de Gennes equations read[37, 42]

$$\left[-\frac{\nabla^2}{2} + V_{KS}(\mathbf{r}) - \mu\right]u_i(\mathbf{r}) + \int d\mathbf{r}' \Delta_s(\mathbf{r}, \mathbf{r}')v_i(\mathbf{r}') = \tilde{E}_i u_i(\mathbf{r}) \quad (11)$$

$$-\left[-\frac{\nabla^2}{2} + V_{KS}(\mathbf{r}) - \mu\right]v_i(\mathbf{r}) + \int d\mathbf{r}' \Delta_s^*(\mathbf{r}, \mathbf{r}')u_i(\mathbf{r}') = \tilde{E}_i v_i(\mathbf{r}) \quad (12)$$

where  $u_i(\mathbf{r}), v_i(\mathbf{r})$  are the particle and hole amplitudes.

We notice here that the non-local nature of the pairing field  $\Delta_s(\mathbf{r}, \mathbf{r}')$  in the above equations does not lead to the ultra-violet divergence in the anomalous density matrix elements which may occur[43, 44] when using, instead of Eq.(11,12), the standard Hartree-Fock Bogoliubov-de Gennes equations of the BCS mean-field theory of superconductivity [45] with a local pairing field  $\Delta_s(\mathbf{r})$ .

The amplitudes  $u_i(\mathbf{r}), v_i(\mathbf{r})$  can be expanded in the complete set of wavefunctions  $\{\phi_i(\mathbf{r})\}$  of the normal-state Kohn-Sham equations:

$$\left[-\frac{\hbar^2}{2M}\nabla^2 + V_{KS}(\mathbf{r}) - \mu\right]\phi_i(\mathbf{r}) = \epsilon_i \phi_i(\mathbf{r}) \quad (13)$$

Within the so-called "decoupling approximation"[37, 46], i.e. assuming  $u_i(\mathbf{r}) \sim u_i \phi_i(\mathbf{r})$  and  $v_i(\mathbf{r}) \sim v_i \phi_i(\mathbf{r})$  (with  $u_i$  and  $v_i$  complex constants), one can write  $\tilde{E}_i = \pm E_i$ , where

$$E_i = \sqrt{\xi_i^2 + |\Delta_i|^2} \quad (14)$$

and  $\xi = \epsilon_i - \mu$

By defining the matrix elements:

$$\Delta_i = \int d\mathbf{r} \int d\mathbf{r}' \phi_i^*(\mathbf{r}) \Delta_s(\mathbf{r}, \mathbf{r}') \phi_i(\mathbf{r}') \quad (15)$$

one can write the following equations for the normal and the anomalous densities:

$$n(\mathbf{r}) = \frac{1}{2} \sum_i \left[1 - \frac{\xi_i}{E_i} \tanh(\beta E_i/2)\right] |\phi_i(\mathbf{r})|^2 \quad (16)$$

$$\chi(\mathbf{r}, \mathbf{r}') = \frac{1}{2} \sum_i \frac{\Delta_i}{E_i} \tanh(\beta E_i/2) \phi_i(\mathbf{r}) \phi_i^*(\mathbf{r}') \quad (17)$$

Using Eq.(10) and (15) one can write Eq.(17) as an implicit equation for  $\Delta_i$ :

$$\Delta_i = \frac{1}{2} \sum_j \frac{\Delta_j}{E_j} \tanh(\beta E_j/2) \int d\mathbf{r} \phi_i^*(\mathbf{r}) \phi_j^*(\mathbf{r}) A_{ij}(\mathbf{r}) \quad (18)$$

where

$$A_{ij}(\mathbf{r}) \equiv \int d\mathbf{r}' \phi_i(\mathbf{r}') \phi_j^*(\mathbf{r}') V_{IL}(|\mathbf{r} - \mathbf{r}'|) \quad (19)$$

The convolution integrals appearing in  $A_{ij}(\mathbf{r})$ , which are the most time consuming step in solving the gap equation (18), are efficiently performed by using Fast Fourier transforms[41], knowing that the Fourier transform of  $V_{IL}(r)$  is

$$V_{IL}(q) = -d^2 q e^{-\lambda q} \quad (20)$$

The actual calculations of the superfluid quantities are performed as follows: (i) first the ground-state density  $n(\mathbf{r})$  and the effective potential  $V_{KS}$  are found by self-consistently solving the Eq.(13) for the occupied states  $\{\phi_i(\mathbf{r}), i = 1, N\}$ ; (ii) a larger number  $N'$  (whose minimum value necessary for converged results depends on the effective coupling between the layers, i.e. on the interlayer distance  $\lambda$ ) of orbitals  $\{\phi_i(\mathbf{r}), i = 1, N'\}$  are calculated in the effective potential  $V_{KS}$  obtained from the previous step; (iii) the number density equation (16) is solved for  $\mu$  using the normalization condition  $\int n(\mathbf{r}) d\mathbf{r} = N$ ; (iv) the gap equation (18) is then solved iteratively to provide  $\Delta_i$ .

The pairing gap  $\Delta_0$  separating the normal to superfluid state is finally found as

$$\Delta_0 = \min_{\{E_i\}} \Delta_i$$

In the BCS regime ( $\mu > 0$ ) the pairing gap  $\Delta_0$  equals  $\Delta_i(\epsilon_F)$ .

Step (ii) in the sequence described above typically requires the (non self-consistent) calculations of a very large number (up to a few thousands) of empty states  $\phi_i$ . Most of the computer time during this step is spent in the G-S process. To expedite this time-consuming part of the calculations, I employed a Block Gram-Schmidt orthogonalization procedure which can be recast using BLAS-3 level matrix-matrix multiplication operations[47], which can be efficiently performed using cpu-optimized mathematical libraries. This allows to speed up the calculation by a factor between 4 to 5 with respect to the time spent doing the conventional G-S iteration, which uses much less efficient BLAS-1 level operations.

From the calculated KS orbitals  $\{\phi_i(\mathbf{r}), i = 1, N'\}$  the condensate number of Fermi pairs can also be easily computed, being defined as follows:

$$n_c = \int d\mathbf{r} \int d\mathbf{r}' |\chi(\mathbf{r}, \mathbf{r}')|^2 = \frac{1}{4} \sum_i \frac{|\Delta_i|^2}{E_i^2} \tanh^2(\beta E_i/2) \quad (21)$$

### III. RESULTS AND DISCUSSION

I will first discuss the case of the *homogeneous* bilayer of dipolar fermions, both at  $T=0$  and at finite temperatures: a comparison with the accurate DMC results at  $T=0$  will allow to assess the accuracy of the method employed here, which will be used in the following Section to address the more complex case of the *inhomogeneous* bilayer system.

I assume in the following calculations  $d = 0.8$  Debye, which is appropriate to  $K_{40}Na_{23}$  molecules in the experimental realization of Ref.[5]. The mass  $M$  is that of a  $K_{40}Na_{23}$  molecule. The spatial range of the potential is thus given by  $r_0 = Md^2/\hbar^2 \sim 0.6 \mu m$ . The adimensional interaction strength characterizing the system is  $k_F r_0$ . I will consider here a fermion density such that  $k_F r_0 = 0.5$  (a relatively weak value which can easily be achieved in experiments), which is the case studied in the  $T=0$  DMC calculations reported in Ref.38 and Ref.24. These results represent a solid benchmark with which the results discussed in the present paper will be compared, at least for the homogeneous system at  $T=0$ . For such value of  $k_F$  the interparticle distance  $\langle r \rangle$  is larger than the range of the interaction, being  $\langle r \rangle / r_0 \sim 3.6$  (dilute system).

#### IIIA. HOMOGENEOUS SYSTEM

The calculated values of the pairing gap  $\Delta_0$  and chemical potential  $\mu$  for the homogeneous bilayer are shown, as a function of the temperature, in Fig.(1). The temperature at which  $\Delta_0 = 0$  is by definition the superfluid

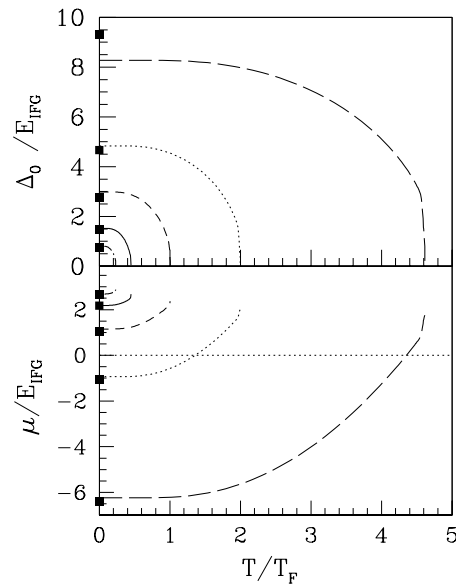


FIG. 1: Pairing gap  $\Delta_0$  (upper panel) and chemical potential  $\mu$  (lower panel) as a function of  $T/T_F$ , in units of  $E_{IFG} = \epsilon_F/2$ , for different values of the interlayer distances:  $k_F\lambda = 0.25$  (dashed line), 0.3 (dotted line), 0.35 (short-dashed line), 0.425 (solid line), 0.5 (dash-dot line). The squares at  $T=0$  show the DMC results from Ref.24.

critical temperature  $T_c$ . I compare these findings at  $T=0$  with the DMC results of Ref.24. Note the excellent agreement throughout the whole BCS-BEC crossover (which is conventionally set at  $\mu = 0$ ). The BEC regime is characterized by negative (large) values of  $\mu$ , whereas in the BCS regime of weak coupling  $\mu > 0$ .

Although the agreement with the  $T=0$  DMC results for the chemical potential is not unexpected since two important ingredients in the effective potential (9) are fitted to DMC data (namely the inter- and intra-layer correlation contributions), the results for the pairing gap, even at  $T=0$ , truly represent a prediction of the KS-DFT theory used here. The calculated values for the gap show nonetheless a discrepancy for  $k_F\lambda = 0.25$ , when compared with the DMC result. I must recall, however, that according to Ref.24 this value for the pairing gap have been computed using a different, approximate, expression than that used for larger values of  $k_F\lambda$ .

From the calculated values of  $\mu$  vs.  $k_F\lambda$  at  $T=0$  I find that the BCS-BEC crossing  $\mu = 0$  occurs at  $k_F\lambda = 0.322$ , in almost perfect agreement with the DMC result,  $k_F\lambda = 0.325$ .

In Fig.(2) the calculated condensate fraction  $n_c$  is shown up to the superfluid critical temperature, for different values of the interlayer distances. As expected, the condensate fraction decreases, as well as the critical

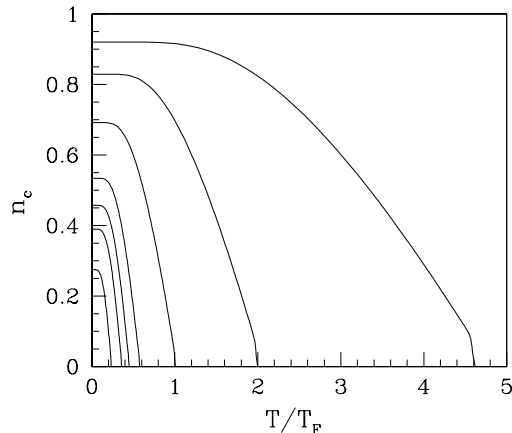


FIG. 2: Condensate fraction of the homogeneous bilayer, for different values of  $k_F \lambda$ . From top to bottom:  $k_F \lambda = 0.25, 0.3, 0.35, 0.4, 0.425, 0.45, 0.5$

temperature, as the system evolves from BEC to BCS regime.

The condensate fraction at  $T=0$ , calculated using Eq.(21), is shown in Fig.(3) as a function of the interlayer distance.

In the BCS region (i.e. for weak coupling resulting from larger interlayer distance) the superfluid fraction  $n_s$  can be calculated using Landau's formula[48] for a two-dimensional system,  $n_s = n - n_n(T)$ , where the normal fluid component (assuming purely fermionic excitations) is given by

$$n_n(T) = \frac{\hbar^2 \beta}{2M} \int \frac{d^2 k}{(2\pi)^2} k^2 \frac{e^{\beta E_k}}{(e^{\beta E_k} + 1)^2} \quad (22)$$

$E_k$  represents the single-particle excitation spectra, which I write here as  $E_k = \sqrt{[\hbar^2 k^2 / 2M^* - \mu]^2 + \Delta_0^2}$ , using the effective mass  $M^*$  as an adjustable parameter. By imposing that the superfluid fraction goes to zero at the calculated critical temperature  $T_c$ , I find  $M^* = 0.7(0)M$ , in reasonable agreement with the effective mass  $M^* = 0.77M$  as computed in Ref.24 using DMC. The calculated superfluid fraction, for  $k_F \lambda = 0.45$  (i.e. in the BCS regime), is compared in Fig.(4) with the condensate fraction for the same interlayer distance.

Finally, the critical superfluid transition temperature is shown with a solid line in Fig.(7). It is known that in 2D the transition from normal to superfluid state is of the Kosterlitz-Thouless (KT) type. However, at least

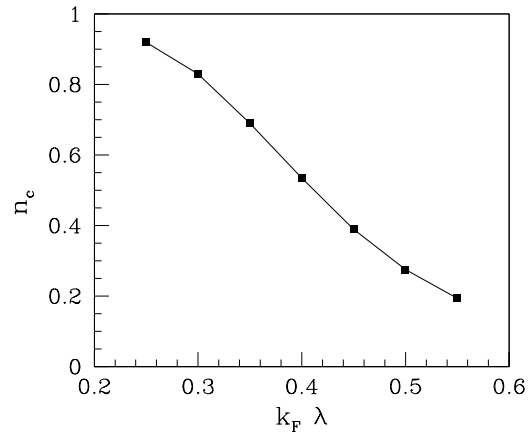


FIG. 3: Condensate fraction of the homogeneous bilayer at  $T = 0$  as a function of the interlayer distance.

in the BCS limit, the KT transition temperature is very close to the one calculated using BCS theory[21]. In the present case this is indeed true on the BCS side of the phase diagram. I computed  $T_{KT}$  through the Kosterlitz-Nelson condition:

$$k_B T_{KT} = \frac{\hbar^2 \pi}{8m} n_s(T_{KT}) \quad (23)$$

and indeed found that it almost coincides with  $T_c$  down to the  $\mu = 0$  line.

### IIIB. INHOMOGENEOUS SYSTEM

I consider in the following a bilayer of 2D dipolar fermions under the effect of an additional external potential in the KS equations (13) corresponding to a square 2D optical lattice

$$V_{ext}(\mathbf{r}) = V_0 [\sin^2(x\pi/a) + \sin^2(y\pi/a)] \quad (24)$$

where two different well depths will be considered in the following, i.e.  $V_0 = 3.52 \epsilon_F$  and  $V_0 = 9.39 \epsilon_F$ . For the sake of simplicity, I will refer in the following to the first case as a "weak" potential, while the second will be termed "strong". The chosen lattice constant is  $a = 2.5 k_F^{-1}$ .

I will consider in the following the case of half-filling (i.e. one fermion every two lattice sites).

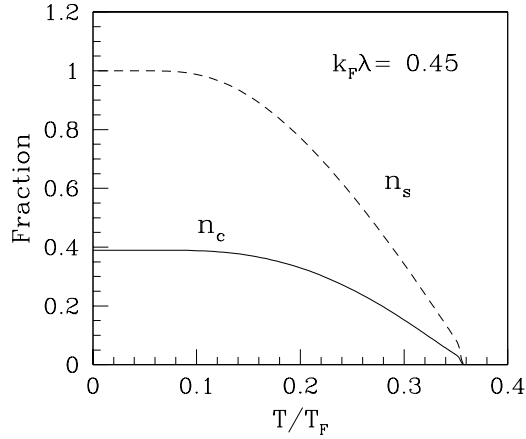


FIG. 4: Condensate (lower curve) and superfluid (upper curve) fraction as a function of temperature.

The chemical potential is calculated as described in Section II as a function of the interlayer separation  $\lambda$ . The results are shown in Fig. (5), where they are compared with the results for the homogeneous bilayer treated in the previous Section. It appears that for stronger confining potentials the BCS-BEC crossover moves towards lower values of the interlayer distance, i.e. it occurs for higher values of the interlayer coupling, and the transition between BCS and BEC regime becomes sharper. The inset shows the fermion density profiles for the two values  $V_0$  of the amplitude of the optical potential considered here, along a line passing through adjacent potential minima.

The condensate fraction is also shown, as a function of the system temperature, in Fig. (6), where it is compared with the homogeneous bilayer results.

Finally, the dependence of the calculated critical superfluid temperatures on the interlayer distance is shown for the two optical potential strengths studied here (and for the homogeneous system as well) in Fig. (7). Notice that in the BCS regime the critical temperature in the presence of a strong optical potential is quite enhanced with respect to the homogeneous system, the enhancement increasing as one goes deeper into the BCS regime. This finding is consistent with similar results found for a different systems of fermionic atoms subject to optical potentials, which undergo a phase transition to a superfluid state at a strongly increased transition temperature with respect to the uniform case [49].

I end this Section by mentioning a transition which

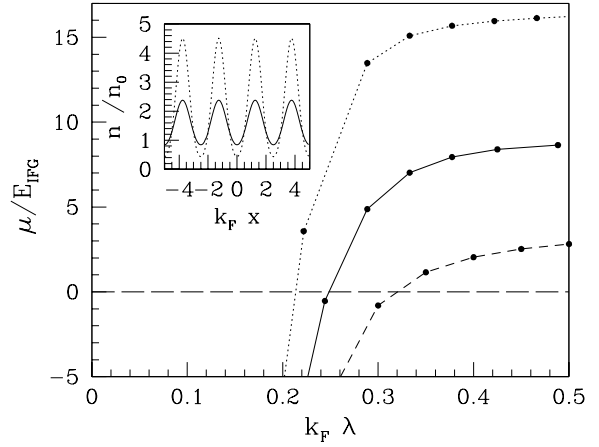


FIG. 5: Chemical potential as a function of the interlayer distance, for the homogeneous system (dashed line), the "weak" potential (solid line) and the "strong" potential (dotted line). The inset shows the fermion density profiles, along the  $x$ -direction, for the two optical potential strengths described in the text:  $V_0 = 3.52 \epsilon_F$  (solid line),  $V_0 = 9.39 \epsilon_F$  (dotted line). Here  $n_0$  is the density of the uniform system.

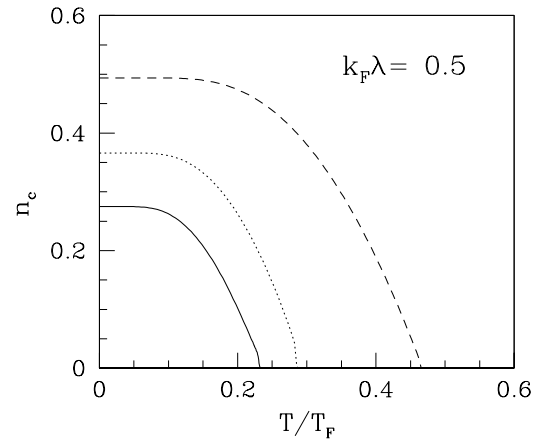


FIG. 6: Condensate fraction for the homogeneous bilayer system (solid line) and for the two values of the strength  $V_0$  of the optical potentials: "weak" potential (dotted line) and "strong" potential (dashed line).

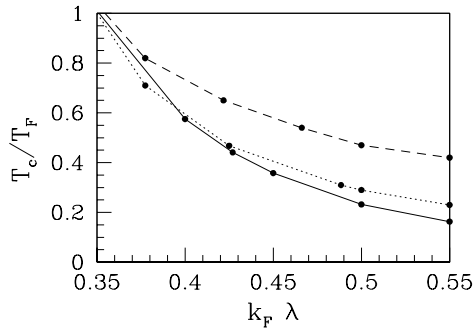


FIG. 7: Calculated critical temperatures for the homogeneous system (solid line) and for the two values of the strength  $V_0$  of the optical potentials: "weak" potential (dotted line) and "strong" potential (dashed line).

takes place in the presence of the "weak" optical potential, when the distance between the two dipolar layers is reduced until it reaches a critical (small) value  $\lambda_c$ , corresponding to a large and negative value of  $\mu$ , i.e. in the deep BEC regime. Then there occurs a sudden rearrangements of the orbital occupations, so that the fermions that for  $\lambda > \lambda_c$  populate each lattice site with 1/2 filling, become suddenly localized every other lattice site (which become populated by one fermion each) as the critical interlayer distance  $\lambda_c$  is reached.

This transition (which occurs at  $k_F \lambda_c = 0.13$ ) is illustrated by the associated fermion density in the optical lattice immediately before and after it, in Fig.(8) and Fig.(9), respectively. The sudden localization of each fermion in every other lattice site results in a marked change in the total fermion density, which suddenly evolves from a "delocalized" configuration characterized by the lattice constant  $a$  (see Fig.(8)) to a 45°-rotated square lattice structure with a larger lattice constant,  $a' = \sqrt{2}a$  (see Fig.(9)). In this "localized" phase, each dipolar fermion sits in a lattice site just above an equally occupied one in the second layer, thus forming a tightly bound composite boson because of the dipole-dipole head-to-tail attractive interaction. In both phases shown in Fig.(8) and Fig.(9), the calculated condensate fraction is close to 1. This sudden transition is not accompanied by any visible anomaly or discontinuity neither in the chemical potential nor in the superconducting gap or

the condensate fraction as a function of  $k_F \lambda$ . However, I speculate that the resulting system of localized composite bosons is expected to be a superfluid, as a result of the finite overlap between neighboring sites, although the superfluid fraction is expected to be smaller than in the 1/2 filling phase shown in Fig.(8). This is suggested in Fig.(10) where the density profiles along the x-axis are shown for the two structures in Fig.(8) and Fig.(9). Due to the reduced overlap between fermion pairs in the "localized" phase, one should expect, once the condition for this transition is met by varying the interlayer distance, to observe a sudden drop in the superfluid fraction. In a way, the resulting state, being characterized by strong density modulations and a finite superfluid fraction, shares some similarities with a truly "super-solid" phase.

To substantiate quantitatively the above speculations the actual superfluid fraction in both phases shown in Fig.(8) and Fig.(9) should be explicitly computed. The superfluid fraction could be extracted, for instance, from the calculated total momentum of the system under a Galilean boost, as obtained by solving the associated time-dependent equations of motion in the co-moving frame of reference (as done, for example, in Ref.50 for a system of soft-core bosons). Since this is not the main subject of the present paper, I will not do this here.

In a practical, quasi-2D realization of the bilayer geometry studied here the transition discussed above, which involves a sudden evolution of the system from an "itinerant" character associated with the first structure, to a more "insulating" one for the second structure, should be observable in principle by studying the transport properties of the bilayer system trapped inside an optical lattice with underlying harmonic confinement (see, for instance, Ref.51), e.g. by monitoring the center of mass motion of the atomic cloud after a sudden displacement of the harmonic trap minimum. As discussed in Ref.51, systems with high filling are characterized by a slower relaxation towards the equilibrium position. Accordingly, the decrease in the superfluid fraction expected with the transition described here should be signalled by a discontinuity in the observed relaxation time of the displaced clouds.

#### IV. CONCLUSIONS

In this paper I applied a multi-orbital Kohn-Sham 'ab initio' formulation of the Density Functional Theory of BCS superconductivity in condensed matter system, which is known to accurately predict the experimental properties of superconducting materials especially for systems where a theory beyond simple BCS superconductivity is needed, to the study of Fermi gas superfluidity, namely in a bilayer of fermionic dipolar molecules in 2D,



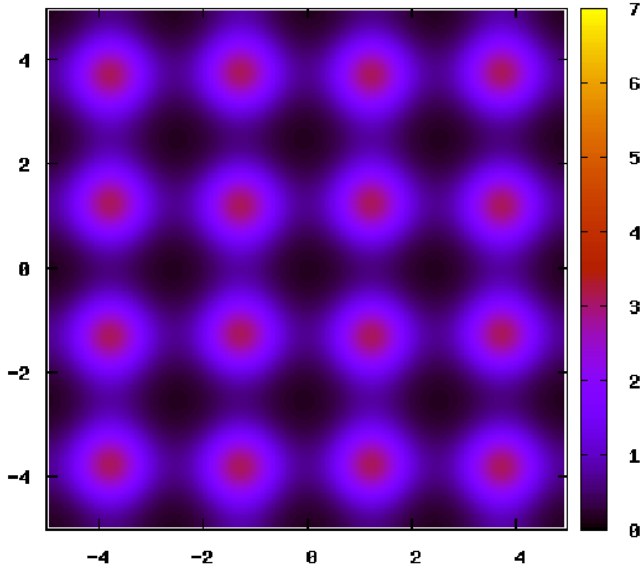


FIG. 8: (Color online) Contour plot of the total density for  $k_F \lambda = 0.12$  in the "weak" optical potential. The coordinates are in units of  $k_F^{-1}$ , while the density is in units of  $n_0$ .

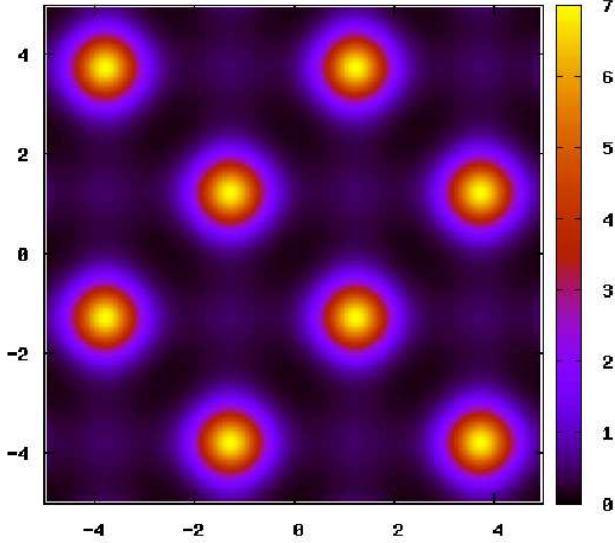


FIG. 9: (Color online) Contour plot of the total density for  $k_F \lambda = 0.14$  in the "weak" optical potential. The coordinates are in units of  $k_F^{-1}$ , while the density is in units of  $n_0$ .

aligned perpendicular to the planes, where the superfluid pairing is provided by the partially attractive interaction between dipoles belonging to different layers.

The finite temperature superfluid properties of both the homogeneous system and one where the fermions in each layer are confined by a square optical lattice have been studied. The resulting  $T=0$  properties of the homogeneous system are found to be in excellent agreement

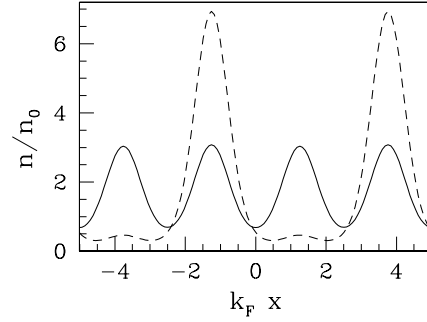


FIG. 10: Density profiles along the x-direction, corresponding to the two structures shown in Fig.(8) and Fig.(9).  $n_0$  is the density of the homogeneous system.

with the results of recent Diffusion Monte Carlo simulations.

I computed the superconducting gap, the condensate fraction and the superfluid transition temperatures, and found how they change as the interlayer distances is varied, together with their dependence upon the depth of the confining optical wells. A marked increase in the superfluid critical temperature in the BCS regime is found with increasing amplitude of the confining potential.

When the distance between the two dipolar layers reaches a critical (small) value, corresponding to coupling strengths characteristic of the deep BEC regime, a transition is observed where the fermions, previously spread out over the lattice, increase their localization such as there is one composite boson in every other lattice site. This transition should be signalled by a sudden drop in the system superfluid fraction, due to the reduced overlap between neighboring particles.

## Acknowledgments

The author thanks Luca Salasnich, Giacomo Bighin, Flavio Toigo, Paolo Umari and Pier Alberto Marchetti for useful discussions and comments.

- 
- [1] B. Svistunov, E. Babaev and N. Prokof'ev, *Superfluid States of Matter*, CRC Press (2015).
- [2] W. Zwerger, Ed., *The BCS-BEC Crossover and the Unitary Fermi Gas*, vol. 836 of Lecture Notes in Physics (Springer, Berlin, 2012).
- [3] S. Giorgini, L.P. Pitaevskii and S. Stringari, Rev. Mod. Phys. **80**, 1215 (2008).
- [4] S. Ospelkaus et al., Science **327**, 853 (2010).
- [5] J.W. Park, S.A. Will and M.W. Zwierlein, Phys. Rev. Lett. **114**, 205302 (2015).
- [6] M.A. Baranov, Phys. Rep. **464**, 71 (2008).
- [7] M.A. Baranov, M. Dalmonte, G. Pupillo and P. Zoller, Chem. Rev. **112**, 5012 (2012).
- [8] Y. Li and C. Wu, J. Phys.: Condens. Matter **26**, 493203 (2014).
- [9] G.M. Bruun and E. Taylor, Phys. Rev. Lett. **101**, 245301 (2008).
- [10] N.R. Cooper and G.V. Shlyapnikov, Phys. Rev. Lett. **103**, 155302 (2009); J. Levinsen, N.R. Cooper and G.V. Shlyapnikov, Phys. Rev. A **84**, 013603 (2011).
- [11] L.M. Sieberer and M.A. Baranov, Phys. Rev. A **84**, 063633 (2011).
- [12] M.M. Parish and F.M. Marchetti, Phys. Rev. Lett. **108**, 145304 (2012).
- [13] M.H.G. de Miranda et al., Nature Phys. **7**, 502 (2011).
- [14] B. Simon, Ann. Phys. **97**, 279 (1976).
- [15] J.R. Armstrong, N.T. Zinner, D.V. Fedorov and A.S. Jensen, Eur. Phys. Lett. **91**, 16001 (2010).
- [16] M. Klawunn, A. Pikovski and L. Santos, Phys. Rev. A **82**, 044701 (2010).
- [17] A. Pikovski, M. Klawunn, G.V. Shlyapnikov and L. Santos, Phys. Rev. Lett. **105**, 215302 (2010).
- [18] M.A. Baranov, A. Micheli, S. Ronen and P. Zoller, Phys. Rev. A **83**, 043602 (2011).
- [19] N.T. Zinner, B. Wunsch, D. Pekker and D.-W. Wang, Phys. Rev. A **85**, 013603 (2012).
- [20] A.C. Potter, E. Berg, D.-W. Wang, B.I. Halperin and E. Demler, Phys. Rev. Lett. **105**, 220406 (2010).
- [21] K. Miyake, Progr. Theor. Phys. **69**, 1794 (1983).
- [22] M. Randeria, J.-M. Duan and L.-Y. Shieh, Phys. Rev. B **41**, 327 (1990).
- [23] S. De Palo, F. Rapisarda and G. Senatore, Phys. Rev. Lett. **88**, 206401 (2002); A. Perali, D. Neilson and A.R. Hamilton, Phys. Rev. Lett. **110**, 146803 (2013).
- [24] N. Matveeva and S. Giorgini, Phys. Rev. A **90**, 053620 (2014).
- [25] P.N. Ma, S. Pilati, M. Troyer and X. Dai, Nature Physics **8**, 601 (2012).
- [26] A. Bulgac, Phys. Rev. A **76**, 040502(R) (2007).
- [27] F. Malet, A. Mirtschink, C.B. Mendl, J. Bjerlin, E.O. Karabulut, S.M. Reimann and P. Gori-Giorgi, Phys. Rev. Lett. **115**, 033006 (2015).
- [28] B.P. van Zyl, W. Kirkby and W. Ferguson, Phys. Rev. A **92**, 023614 (2015).
- [29] B. Fang and B.-G. Englert, Phys. Rev. A **83**, 052517 (2011).
- [30] B.P. van Zyl, E. Zaremba and P. Pisarski, Phys. Rev. A **87**, 043614 (2013).
- [31] B. P. van Zyl, A. Farrell, E. Zaremba, J. Towers, P. Pisarski, and D. A. W. Hutchinson, Phys. Rev. A **89**, 022503 (2014).
- [32] S.H. Abedinpour, R. Asgari, B. Tanatar and M. Polini, Ann. Phys. **340**, 25 (2014); H. Ustunel, S.H. Abedinpour and B. Tanatar, J. Phys. Conf. Ser. **568**, 012020 (2014).
- [33] W. Kohn and L.J. Sham, Phys. Rev. **140**, A1133 (1965).
- [34] S. Pilati, I. Zintchenko and M. Troyer, Phys. Rev. Lett. **112**, 015301 (2014).
- [35] M. Rossi, F. Ancilotto, L. Salasnich and F. Toigo, Eur. Phys. J. **224**, 565 (2015).
- [36] F. Ancilotto, Phys. Rev. A **92**, 061602(R) (2015).
- [37] L.N. Oliveira, E.K.U. Gross and W. Kohn, Phys. Rev. Lett. **60**, 2430 (1988); S. Kurth, M. Marques, M. Liders and E.K.U. Gross, Phys. Rev. Lett. **83**, 2628 (1999); M. Liders, M.A.L. Marques, N.N. Lathiotakis, A. Floris, G. Profeta, L. Fast, A. Continenza, S. Massidda and E.K.U. Gross, Phys. Rev. B **72**, 024545 (2005).
- [38] N. Matveeva and S. Giorgini, Phys. Rev. Lett. **109**, 200401 (2012).
- [39] P. Hohenberg and W. Kohn, Phys. Rev. **136**, B864 (1964).
- [40] F. Ancilotto, D. G. Austing, M. Barranco, R. Mayol, K. Muraki, M. Pi, S. Sasaki, and S. Tarucha, Phys. Rev. B **67**, 205311 (2003).
- [41] M. Frigo and S.G. Johnson, Proc. IEEE **93**, 216 (2005).
- [42] N.N. Bogoliubov, Sov. Phys. JETP **7**, 41 (1958).
- [43] A. Bulgac, Phys. Rev. C **65**, 051305(R) (2002).
- [44] G. Bruun, Y. Castin, R. Dum and K. Burnett, Eur. Phys. J. D **7**, 433 (1999).
- [45] D.M. Eagles, Phys. Rev. **186**, 456 (1969); A.J. Leggett, *Modern Trends in the Theory of Condensed Matter*, edited by A. Pekalski and J. Przystawa (Springer, Berlin, 1980).
- [46] M. Liders, PhD thesis, Bayerische Julius-Maximilians-Universität (Würzburg, 1995).
- [47] P. Umari, private communication.
- [48] A.L. Fetter, Rev. Mod. Phys. **81**, 647 (2009).
- [49] W. Hofstetter, J.I. Cirac, P. Zoller, E. Demler and M. D. Lukin, Phys. Rev. Lett. **89**, 220407 (2002).
- [50] F. Ancilotto, M. Rossi and F. Toigo, Phys. Rev. A **88**, 033618 (2013).
- [51] N. Strohmaier, Y. Takasu, K. Guenter et al. Phys. Rev. Lett. **99**, 220601 (2007).
- [52] M. Greiner, O. Mandel, T. Esslinger, T.W. Hansch and I. Bloch, Nature **415**, 39 (2002).